Towards a non-invasive monitoring of the soil-plant-atmosphere interactions: insights from a Mediterranean vineyard case study

Riccardo Mazzoleni
riccardo.mazzoleni2@unibo.it
University of Bologna
Francesco Vinzio
University of Bologna
Marco Benfenati
University of Bologna
Ilaria Filippetti
University of Bologna
Gabriele Baroni
University of Bologna

Research Article

Keywords:

Posted Date: December 15th, 2025

DOI: https://doi.org/10.21203/rs.3.rs-7981024/v1

Additional Declarations: No competing interests reported.

Towards a non-invasive monitoring of the soil-plant-atmosphere interactions: insights from a Mediterranean vineyard case study

Riccardo Mazzoleni[1], Francesco Vinzio[1], Marco Benfenati[1], Ilaria Filippetti[1], Gabriele Baroni[1]

[1]Department of Agricultural and Food Sciences (DISTAL), University of Bologna, Viale Giuseppe Fanin 42-50, 40127 Bologna, Italy.

Correspondence to: Riccardo Mazzoleni (riccardo.mazzoleni2@unibo.it)

Abstract. This study evaluated a non-invasive, integrated monitoring approach to characterize the soil-plant-atmosphere continuum (SPAC) in a commercial vineyard of Pignoletto (PG) and Trebbiano Romagnolo (TR). The approach is based on a cosmic-ray neutron sensor (CRNS) to continuously monitor soil water content (SWC), which was normalized into extractable soil water (ESW) to represent plant-available water. Moreover, vapor pressure deficit (VPD) was calculated based on weather data to characterize the atmospheric demand. Finally, remotely sensed NDVI data were used to detect canopy development and vine physiological responses. Over two growing seasons, measurements of midday stem water potential (Ψ_{stem}) and berry composition complemented the monitoring activities. In 2023, ripening was largely buffered from atmospheric demand, with Ψ_{stem} values between -0.66 and -1.06 MPa, reflecting SWC as a non-limiting factor and uniform ripening. Conversely, the 2024 season showed more negative Ψ_{stem} (-0.95 to -1.12 MPa) and an accelerated ripening process, particularly in TR. Principal Component Analysis (PCA) explained 65% of the variance in 2023 and 81.5% in 2024, revealing that environmental drivers (ESW, VPD) became more tightly linked to physiological and grape composition traits (Ψ_{stem}, TSS, TA). Overall, the results showed the capability of the integrated approach to capture the main interactions within the SPAC, offering a non-invasive and scalable tool for supporting precision and sustainability in Mediterranean viticulture.

Introduction

In the Mediterranean basin, efficient water use has become a critical concern due to increasing climatic variability, especially considering the recurrent summer droughts (Büntgen et al., 2024; Seager et al., 2014). In this context, precision agriculture has emerged as a transformative approach in modern agriculture, seeking to optimize crop production and minimize input and costs. Beside, precision agriculture offers promising strategies to enhance sustainability, highlighting the central importance of irrigation management (Bwambale et al., 2022). This is especially relevant in vineyard, where operations depend significantly on effective water management, as water availability can notably impact grape quality and yield (Fuentes and Gago, 2022). In vineyards, for instance, water availability needs to be tailored based on the intended use of the grapes (Bonada et al., 2023), as under a moderate water deficit during the fruit development, it produces grapes with high quality potential for winemaking (Acevedo-Opazo et al., 2010).

In this scenario, soil water content (SWC) is a crucial variable in the soil-plant-atmosphere continuum (SPAC), influencing not only the evapotranspiration process but also being strictly correlated with vine stress and growth (Pellegrino et al., 2005; Seneviratne et al., 2010). Water use in vineyards is a function of available water content of the soil (Lebon et al., 2003), and the occurrence of low SWC may trigger reductions in vegetation productivity driven by drought and heat (Zhou et al., 2019), a scenario particularly critical during the grapes ripening period. Grapevine, although is considered to be highly adaptable to water restrictions (Lovisolo et al., 2010), exhibit however complex physiological responses to water deficits that can influence both vegetative growth and fruit development (Chaves et al., 2010; Valentini et al., 2022). Rainfall during the growing season is often inadequate to meet vine water requirements, making supplemental irrigation increasingly essential. Applied during key phenological stages such as veraison and ripening, irrigation is therefore recognized as an effective adaptive strategy to counteract the negative effects of summer multiple stresses (Allegro et al., 2023).

Given this, the continuous and accurate monitoring of SWC becomes essential for preventing water stress condition and programming irrigation. Numerous methods for assessing SWC, ranging from point-scale to satellite remote sensing approaches have been devised (Susha Lekshmi et al., 2014).The former has been widely used but applicability and interpretation of the results is limited due to the inherent strong spatial variability of the soil-plant system (Soulis et al., 2015). The latter, even if it has shown an increasing adaptability, it is currently constrained by the relatively small size of the agricultural management units, e.g., lower than 1 km^2 (Massari et al., 2021). Ultimately, research interest was focused on the development and application of non-invasive proximal sensors based on cosmic-ray neutron sensing (CRNS). This approach relies on the inverse relation between neutrons generated by cosmic-ray fluxes and the existence of hydrogen, primarily present in the soil as in the water molecule. Moist soils strongly decelerate and absorb neutrons, leading to a reduced neutron flux at the detector. Conversely, in drier soils, fewer neutrons are absorbed, resulting in a higher detected neutron intensity (Zreda et al., 2008). CRNS probes are installed above the soil surface allowing non-invasive moisture measurements, with a penetration depth ranging from 10 cm to 40 cm and a radius of influence ranging from 100 m to 200 m (Köhli et al., 2015; Schrön et al., 2017). Recent advancements in sensor implementation have enabled the utilization of CRNS probes to monitor SWC fluctuations in agricultural fields, particularly in response to irrigation interventions (Brogi et al., 2023; Gianessi et al., 2024; Mazzoleni et al., 2025). However, the ongoing debate surrounding the use of CRNS for precision irrigation continues to captivate attention, with studies on the topic remaining limited (Li et al., 2019).

In this context, combining CRNS-based SWC monitoring with additional weather-based and plant-based indicators can offer a powerful approach to monitor the SPAC and to assess grapevine growth (add). Along with soil moisture observations, the monitoring of the atmosphere demand such as vapour water deficit (VPD) showed in fact to better capture the co-regulation of crop water stress (Novick et al., 2016; J. Zhang et al., 2021). In addition, plant-based measurements provided the key feature to quantify the on-set of the stress and the effect on vegetation growth (add). In this case, among the different techniques, (Velazquez-Chavez et al., 2024), Normalized Difference Vegetation Index (NDVI) detected by satellite has been widely applied and has become a validated tool to reflect spatio-temporal patterns in vine vigour, water stress, and grape quality (Giovos et al., 2021). For instance, Bolognini et al. (2023) demonstrated that NDVI data from Sentinel-2, collected at key phenological stages in Sangiovese vineyards, could effectively define zones with distinct levels of crop water stress, yield, and grape quality. Pereyra et al. (2022) used NDVI to delineate vigor-based zones in vineyards, enabling variable-rate irrigation and canopy management that led to improved yield and berry composition. Similarly, Ortuani et al. (2024) compared UAV and Sentinel-2-derived NDVI in vineyards in northern Italy, showing that even with coarser resolution, satellite imagery reliably captured the main patterns of variability relevant to vineyard management.

Building on previous work that validated the use of CRNS for SWC monitoring in vineyards (Mazzoleni et al., 2025), this study takes a step further by evaluating its functional integration with plant and atmosphere-based indicators. Rather than focusing solely on SWC dynamics, the analysis seeks to understand how temporal fluctuations in extractable soil water (ESW) interact with atmospheric demand and drive physiological responses in the vine, as expressed by midday stem water potential (Ψ_{stem}) and berry composition parameters. To test this, ESW derived from CRNS was integrated with VPD and remote sensing NDVI, allowing for a combined, non-invasive assessment of soil-plant-atmosphere interactions. The overarching goal is to evaluate the actual contribution and complementarity of these measurements, identifying which indicators are most informative, and how their integration can strengthen irrigation strategies in Mediterranean viticulture.

Materials and methods

Study site overview and setup description

The vineyard (*Vitis vinifera* L.), planted with cv. Trebbiano Romagnolo (TR) and cv. Pignoletto (PG), is located at Imola, Bologna, Italy (44.384954, 11.698439), covering an approximate area of 12 hectares (Fig. 1). The vine rows were oriented northeast to southwest, trained to a vertical shoot positioned spur-pruned cordon, and spaced at 1 m within the row and 2.5 m between rows.

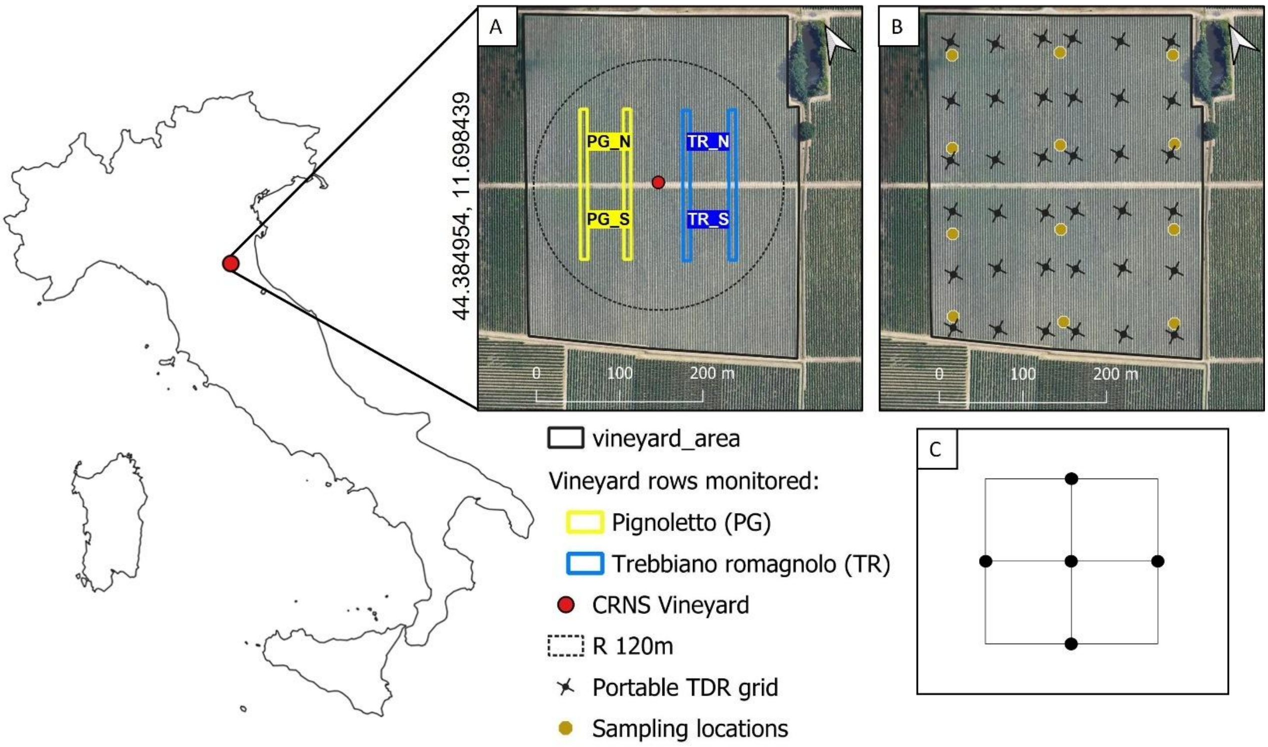

Fig. 1 Overview of the experimental vineyard site showing its location in Italy with geographic coordinates and the layout of the instrumentation and sampling design. (A) CRNS sensor installation point and subdivision of monitored vineyard rows between the two cultivars, Pignoletto (PG, yellow) and Trebbiano romagnolo (TR, blue), with corresponding north and south blocks for each variety. R = 120 m indicates the extent of the CRNS detection footprint. (B) Scheme of soil sampling and monitoring layout: 12 locations for soil texture analysis (yellow circles) and grid of portable TDR measurement points (black crosses). (C) Detail of a single TDR measurement location, where five repeated readings were taken per point.

Irrigation within this area was provided with a sub-surface drip irrigation (SDI) system, and was managed by Società Agricola CACI in Imola, Bologna (Italy). The SDI system is placed at a depth of 25 cm along two lines parallel to each row of plants, and drip system has a water capacity of 0.008 $m^3 h^{-1}$. Irrigation events and total volume distributed (mm d^{-1}) during the two seasons monitored, together with grape phenological phase (BBCH) according to Lorenz et al. (1995), are resumed in Table 1.

Table 1 Irrigation schedule and estimated phenological stages (BBCH scale) during the 2023 and 2024 growing seasons. Phenological stages were estimated based on field observations, covering berry development (BBCH 75-79), onset of ripening (veraison; BBCH 81-83), and berry maturation (BBCH 85-89).

Irrigation event (DOY)	2023	205	212	222	229	240	259	2024	194	202	209	214	218	233
Total volume distributed (mm d^{-1})		20	18	16	18	16	16		20	18	18	18	18	18
Estimated BBCH stage		75-77	77-79	81-83	83-85	85-87	87-89		75-77	77-79	81-83	83-85	85-87	87-89

Soil characterization and environmental variables

To assess soil physical variability across the vineyard, twelve samples were collected from predefined locations evenly distributed across all sub-parcels, ensuring coverage both along rows and across transects (Fig. 1 B). Sampling points were spaced 100 m apart within transects and 130 m between vine rows. Soil samples were taken at 0-50 cm depth using a manual auger and stored in sealed aluminium trays for lab analysis. Particle size distribution (PSD) was determined with a PARIO™ system (METER Group, Pullman, WA, USA), which automatically implements Stokes' Law within the 2-63 µm range to generate continuous PSD curves. Precipitation and weather data were sourced from the network stations of the regional environmental agency ARPAe and were processed following Antolini et al. (2016). Based on these data, the VPD was calculated according to Allen et al. (1998) on an hourly basis for both season.

Soil water content monitoring

A CRNS probe manufactured by Finapp S.p.a (Montegrotto Terme, Padova, Italy) was installed on April 2023 (Fig. 1 A). According to Stevanato et al. (2019), the probe is enriched with few centimeters of polyethylene to moderate and slow down epithermal neutrons and enhance the probe's sensitivity to SWC (Köhli et al., 2015). Following Zreda et al. (2012), the neutrons measured by the CRNS sensor were corrected to account for changing in air pressure, air humidity and variability in the incoming neutron flux. The CRNS sensor calibration took place on DOY 129 in 2023. The procedure for calibrating the CRNS sensor in this site was previously documented by Mazzoleni et al. (2025) and the protocol followed Franz et al. (2012). The calibration procedure allows to convert corrected neutron counts (Nc) into SWC based on the following equation proposed by Desilets et al. (2010):

$$SWC_v(Nc) = \left(\frac{0.0808}{\frac{Nc}{N_0} - 0.372} - 0.115 - SWC_{offset}\right) \cdot \frac{\rho_{bd}}{\rho_w}, \qquad \text{Eq. 1}$$

where ρ_{bd} and ρ_w are respectively the soil bulk density and water density (kg m^{-3}); SWC_{offset} is the contribution of static hydrogen pools (SHP), which is represented by the lattice water (LW) and soil organic carbon (SOC); $SWC_v (N_c)$ is the volumetric SWC average during the calibration day, N_0 is the calibration parameter.

For a better interpretation of the SWC values throughout the season, extractable soil water (ESW) was calculated based on the method of Gerakis and Zalidis (1998), with modifications following Zhang et al. (2012), to better capture the scale and dynamics of plant-available water. ESW was defined as a dimensionless ratio representing the proportion of available water in the soil, calculated using the current SWC relative to the range between field capacity (FC) and wilting point (WP) as follow:

$$ESW = \frac{SWC - WP}{FC - WP},\qquad \text{Eq. 2}$$

where SWC represents the volumetric soil water content measured hourly by CRNS sensor, FC is the field capacity (0.38 m^3m^{-3}) and WP is the wilting point (0.17 m^3m^{-3}). These values were determined by applying prediction algorithms (pedotransfer functions; PTFs) through the web interface of Szabó et al. (2021), utilizing a mix of the soil samples from the textural analysis described in Section 2.2. Additionally, measurements with a portable TDR sensor (Spectrum Technologies, Inc., Aurora, IL, USA) were carried out in 2023 (DOY 128, 158, and 296) and in 2024 (DOY 194), to characterize the spatial variability of soil SWC across the vineyard and to assess the consistency of observed patterns (Fig. 1 B). The sensor allowed mobile, point-scale, repetitive acquisitions of SWC (%), with a vertical resolution of 15 cm depth. Measurements were evenly distributed across all sub-parcels, ensuring coverage both along vine rows and across transects. At each location, five repeated acquisitions were taken (Fig. 1 C), with sampling points spaced 50 m apart within transects and 100 m between vine rows, resulting in approximately 500 individual measurements per survey date.

Plant physiological measurement

The monitored vine rows were divided into two sectors per variety, corresponding to the north and south sections of the vineyard, which are naturally separated by a field road. This subdivision allowed for a more detailed analysis of intra-varietal and spatial variability. Accordingly, the grape varieties are referred to as PG_N and PG_S for Pignoletto, and TR_N and TR_S for Trebbiano Romagnolo (Fig. 1 A). A total of 80 vines were randomly selected from the monitored vine rows, 20 in each sector. These vines were monitored throughout the 2023 and 2024 growing seasons to assess their water status and berry composition.

Vine water status was evaluated during both the 2023 and 2024 growing seasons on three dates per year (DOY 201, 215, and 222 in 2023; DOY 194, 218, and 234 in 2024). Measurements were taken at solar midday by determining stem water potential (Ψ_{stem}) with a Scholander pressure chamber (Soilmoisture Corp., Santa Barbara, CA, USA). For each date, a total of 24 leaves were randomly sampled from the vines selected for each variety, 12 in each sector. The leaves were covered with aluminum foil and placed in a plastic bag for 45 minutes prior to measurement.

From each of the 20 selected vines per sector, 50 berries were randomly collected on multiple dates prior to harvest and at harvest. In 2023, sampling occurred on DOY 222, 234, 243, and 249, while in 2024, it was conducted on DOY 220, 235, and 241. The following parameters were analyzed: berry weight (g), total soluble solids (°Brix) using a temperature-compensated refractometer (Misure Maselli, Parma, Italy), and must pH and titratable acidity (g L^{-1}), measured with an automatic titrator (Crison Instruments, Barcelona, Spain). In addition, the overall yield at harvest for both varieties was considered to provide a broader context for vine productivity.

Remote sensing data

NDVI maps were generated using level-2A reflectance products from the Sentinel-2 satellite. Data processing and analysis were performed on the Google Earth Engine (GEE) cloud-based platform. Available imagery from the years 2023 and 2024 was first filtered to include only acquisitions captured during the vines growing season, between May 1st and October 1st of each year. Subsequently, the Scene Classification Layer (SCL), provided by the European Space Agency (ESA), was used to generate a filtering mask, which was then applied to the selected images: pixels not classified as vegetation (Class 4) or bare soil (Class 5) were removed. It is well established that the Sen2Cor algorithm, used to elaborate the SCL products, is not always effective in detecting all kinds of cloud coverage, especially close to clouds margins (Baetens et al., 2019). For this reason, images with more than 10% of invalid pixels were also excluded from the analysis. Lastly, a mobile window filter was applied to the mean-values time series, to remove outliers. In the end, a total of 32 acquisitions were used: 17 images from 2023 and 15 from 2024.

Data processing and statistical analysis

The soil textural composition (% of clay, silt, and sand) for each sample, as well as the individual acquisitions of SWC (%) with the portable TDR, were processed using QGIS (LTR version 3.34.10 - Prizren) and interpolated using the Inverse Distance Weighting (IDW) method to generate spatial distribution maps for visual representation. All data processing and statistical analyses were performed using software R, in RStudio (2024.12.1+563 "Kousa Dogwood" Release), employing specific packages according to the analysis type: *ggplot2* (Wickham, 2011) for the graphs and plots*, lubridate* (Grolemund & Wickham, 2011) to manage temporal data*, FactoMineR* (Lê et al., 2008) and *factoextra* (Kassambara and Mundt, 2016) for multi-variate analysis. For the latter, all variables were standardized (z-scores) and subjected to Principal Component Analysis (PCA) to identify the main gradients of variation and the relative contribution of environmental drivers and physiological traits. The contribution of each variable to PC1 and PC2 was quantified through loadings, and biplots were generated to visualize relationships among variables and vineyard sectors.

Results

Soil characteristics and intra-field variability

The interpolated soil texture fractions across the vineyard are depicted in Fig. 2. The soil texture ranged from clay loam to clay, with localized sandy inclusions. Clay content exhibited the strongest spatial gradient, with markedly higher values (>50%) in the southern and eastern parts of the vineyard, particularly in correspondence with the TR_S sector, whereas lower percentages were observed in the central area. By comparison, silt showed a narrower range of variation, with slightly higher concentrations in the south-western and north-eastern areas, where the PG_S and TR_N sectors are located, respectively. Sand was the least represented fraction but showed localized accumulation in the western, and especially the south-western, zones encompassing the PG_N and PG_S sectors, where the relatively coarser texture is expected to enhance drainage and reduce water storage capacity.

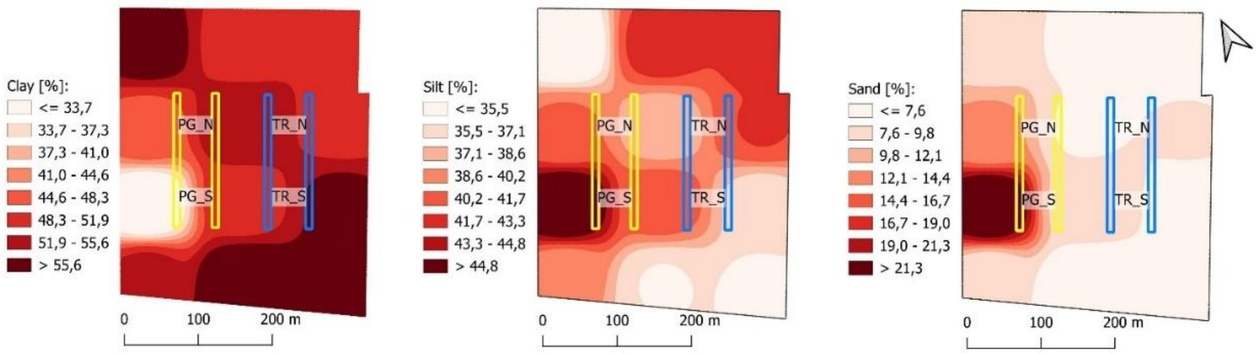

Fig. 2 Spatial distribution maps of soil textural fractions (clay, silt, and sand, %) across the experimental vineyard. Yellow and blue boxes indicate monitored vine rows divided into two sectors per variety (N and S) of cv. Pignoletto (PG) and cv. Trebbiano Romagnolo (TR), respectively.

The spatial distribution of SWC measured with a portable TDR sensor at 15 cm depth across the experimental vineyard is shown in Fig. 3 (A - D). In 2023, early-season measurements (Fig. 3 A, B) indicated generally high SWC (>40%), with relatively homogeneous patterns across sub-parcels, reflecting mostly the substantial rainfall events occurred in May. By late season (Fig. 3 C), SWC decreased markedly, with localized dry patches (<20%) emerging particularly in the western and south-western part of the field, in line with the expectations after the warm and dry summer conditions. In 2024 (Fig. 3 D), the overall pattern was consistent to what observed in the previous year, with contrasting zones ranging from <25% to >45%, highlighting differences in water retention and depletion across sectors, particularly with a western-eastern gradient. When compared with the textural analysis, these patterns are coherent with the underlying soil heterogeneity. Clay-rich zones in the eastern and southern sectors generally coincided with areas retaining higher SWC (%), whereas sandier areas, particularly in the south-western portion where PG_N and PG_S are located, tended to exhibit lower water contents.

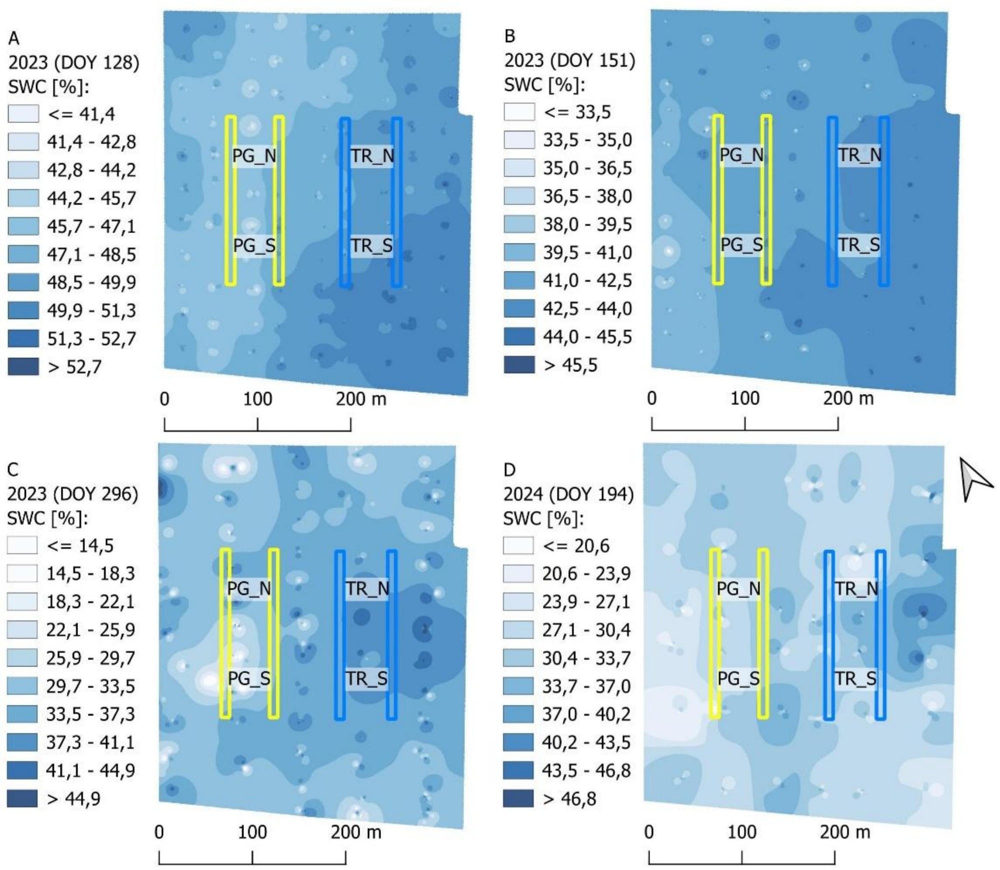

Fig. 3 Spatial distribution of SWC (%) measured with a portable TDR sensor at 15 cm depth across the experimental vineyard. Maps correspond to DOY 128 (A), DOY 151 (B), and DOY 296 (C) of 2023, and DOY 194 (D) of 2024. Data represent ~500 measurements per survey date. Yellow and blue boxes indicate monitored vine rows divided into two sectors per variety (N and S) of cv. Pignoletto (PG) and cv. Trebbiano Romagnolo (TR), respectively.

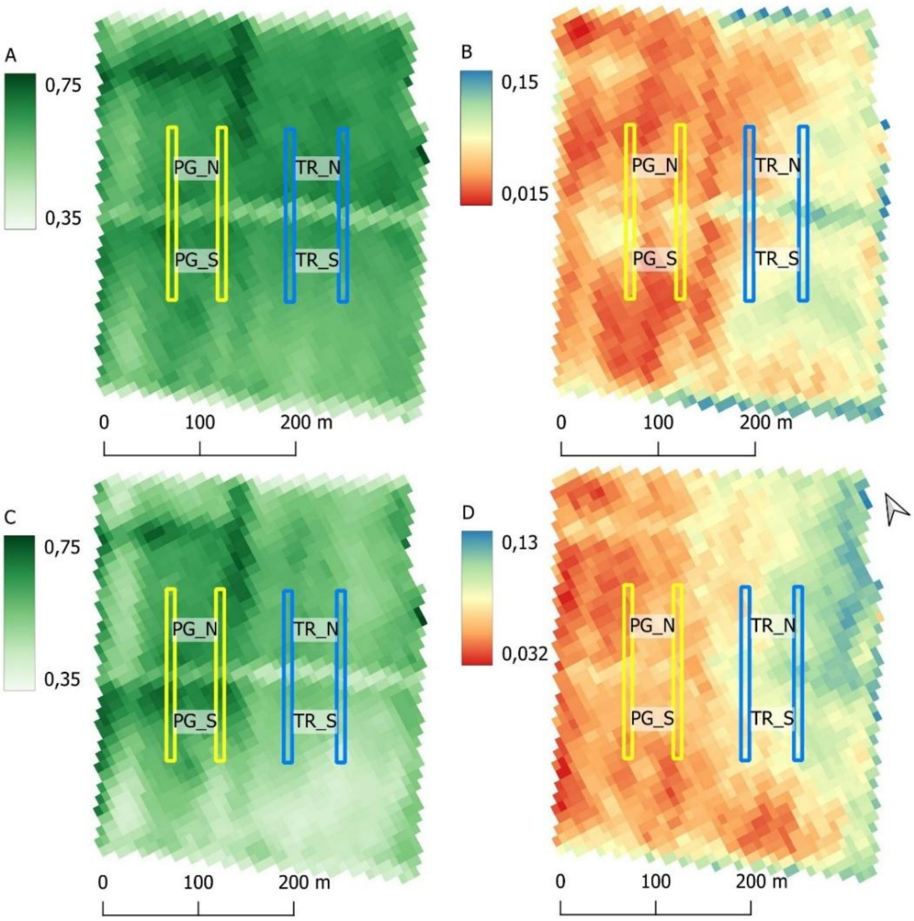

Fig. 4 Spatial distribution of average NDVI values and their seasonal variability across the vineyard during the 2023 and 2024 growing seasons (May 1st to October 1st). (A) Mean NDVI for 2023; (B) standard deviation of NDVI for 2023; (C) mean NDVI for 2024; (D) standard deviation of NDVI for 2024. Yellow and blue boxes indicate monitored vine rows divided into two sectors per variety (N and S) of cv. Pignoletto (PG) and cv. Trebbiano Romagnolo (TR), respectively.

The spatial distribution of average NDVI values and their seasonal variability across the vineyard during the 2023 and 2024 growing seasons are depicted in Fig. 4 (A - D). In 2023, the vineyard exhibited relatively homogeneous average NDVI values across the entire area (Fig. 4 A), with slightly higher values observed in the north-western sectors compared to the south-eastern ones, where NDVI appeared lower. However, the corresponding NDVI standard deviation map (Fig. 4 B) revealed notable intra-field variability, particularly along an east-west gradient. This pattern may reflect spatial differences in vine growth dynamics throughout the season. In 2024, the average NDVI values appeared to be lower compared to the previous season, especially in the south-western zone, corresponding to TR_S (Fig. 4 C). Comparably to the 2023, the trend of NDVI standard deviation appeared even more evident across the east-western gradient (Fig. 4 D).

Seasonal pattern of soil water content and environmental drivers

The seasonal dynamics of soil water status, expressed as both SWC and normalized ESW, atmospheric evaporative demand represented by VPD, water inputs from precipitation and irrigation and daily average on NDVI are illustrated in Fig. 5 (A - H).

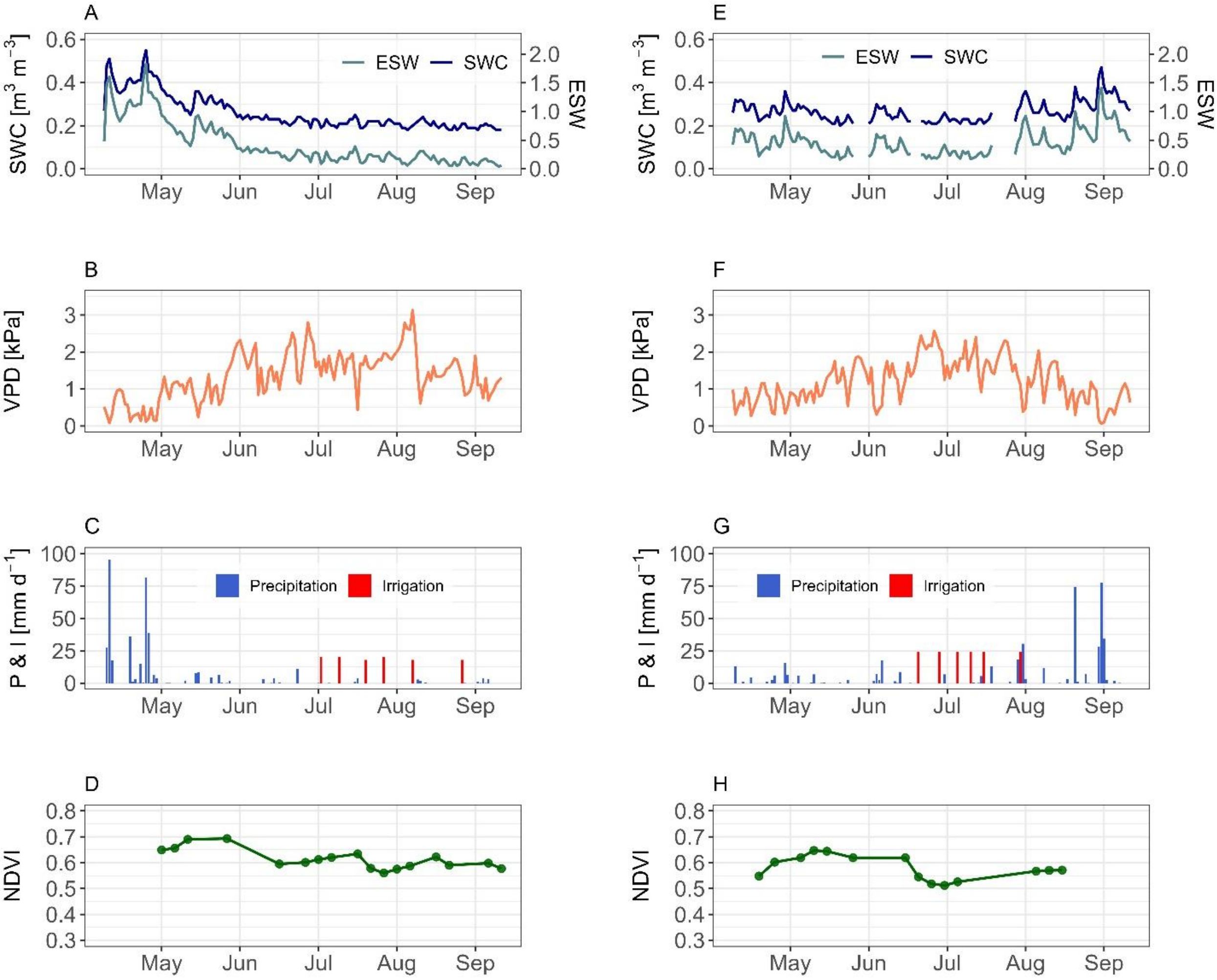

Fig. 5 Seasonal dynamics of the monitored variables to assess the SPAC during the 2023 and 2024 growing seasons. Panels A-D refer to the 2023 season; Panels E-H to 2024. (A, E): daily trends of soil water content (SWC, m^3 m^{-3}) measured with the cosmic-ray neutron sensor (CRNS), and extractable soil water (ESW), normalized between field capacity and wilting point. (B, F): daily vapor pressure deficit (VPD, kPa) trends representing atmospheric evaporative demand. (C, G): daily cumulative precipitation (blue bars) and irrigation volumes (red bars) applied to the vineyard (mm d^{-1}). (D, H): interpolated daily average NDVI values registered across the season.

In 2023 (Fig. 5 A - D), the early season was characterized by abundant precipitation events, with a total cumulative precipitation amounting to approximately 300 mm recorded in the Emilia-Romagna region. Consequently, this led to high values of both SWC and ESW. However, from June onward, a sharp decrease in both SWC and ESW was observed, driven by the simultaneous rise in VPD (Fig. 5 B) and the lack of significant rainfall (Fig. 5 C). Despite some irrigation events starting in July, the overall water availability remained low, as shown by the persistently declining ESW values, which approached critical low values in late summer. NDVI values (Fig. 5 D) were initially high, consistent with the expected canopy vigor at onset of vegetative growth. As the season progressed, NDVI gradually declined and then stabilized around 0.60 - 0.55, reflecting a moderate and steady canopy condition during the summer months. The slight decrease was likely associated with canopy management practices (e.g., shoot trimming) and with the senescence or yellowing of inter-row herbaceous cover, which can influence the spectral signal captured by remote sensing (Palazzi et al., 2023).

During 2024, the overall pattern appeared slightly different (Fig. 5 E - H). Although spring rainfall were less intense but more consistent towards the end of June, irrigation inputs were managed consistently from early July (Fig. 5 G). These inputs helped maintain higher SWC and ESW levels throughout most of the season (Fig. 5 E), despite the VPD following a similar seasonal pattern to 2023, with increasing atmospheric demand from May to August. Similar to the previous year, NDVI values rose in mid to late May (Fig. 5 H) with the onset of vegetative growth, followed by a slight decline during the warmer months.

Vine water status and grape berry development

Results of the vine water status measurements, expressed as midday Ψ_{stem}, and grape berry development are depicted in Table 2 and Fig. 6 (A - H), respectively. In 2023, the Ψ_{stem} range (-0.66 to -1.06 MPa) indicated mild to moderate levels of water stress, consistent across grape varieties, with differences among vineyard sectors generally not statistically significant (Table 2). This suggests a rather uniform vine water status, likely due to more consistent SWC availability or effective irrigation, as previously observed in the Section 3.2, and as it is visible in Table 1.
In contrast, the 2024 measurements revealed more negative Ψ_{stem} values across all dates, consistent with overall higher VPD demand, and despite higher ESW compared to the previous year. Statistical differences among sectors remained limited, while a uniform vine water status was consistent with the previous year. However, a subtle pattern emerged, as PG_S block consistently showed more negative Ψ_{stem} values, particularly on DOY 218 and 234, hinting at a slightly reduced water availability or greater water demand in that block. The observations in the TR_S sector were similar, with slightly significant higher Ψ_{stem} value on DOY 234.
Consistent with the overall midday Ψ_{stem} patterns, berry ripening dynamics also exhibited limited intra-varietal variability in both years (Fig. 6 A - H). Berry weight (Fig. 6 A - E) increased progressively toward harvest, and although average berry size remained comparable between seasons, both varieties showed a decline in yield per hectare in 2024 compared to 2023. Specifically, total yield decreased from 15 $t\ ha^{-1}$ to 13 $t\ ha^{-1}$ for Pignoletto and from 21 $t\ ha^{-1}$ to 18 $t\ ha^{-1}$ for Trebbiano Romagnolo, corresponding to reductions of approximately 13% and 14%, respectively. Sugar accumulation (Fig. 6 B, F) followed a typical linear trend, reaching about 20 °Brix at harvest in both years for both grape varieties.

Table 2 Midday stem water potential (Ψ_{stem}, MPa) measured in Pignoletto (PG) and Trebbiano Romagnolo (TR) vines across four vineyard sectors (N = North, S = South) during the 2023 and 2024 growing seasons. Values represent means of 20 vines per sector. Different letters within each row indicate statistically significant differences among sectors according to Tukey's HSD test ($p < 0.05$).

cv		PG		TR	
Sector		N	S	N	S
2023					
DOY	201	-0.78 a	-0.82 a	-0.72 a	-0.66 a
	215	-0.88 a	-1.06 a	-0.82 a	-0.80 a
	222	-0.74 a	-0.80 a	-0.72 a	-0.66 a
2024					
DOY	194	-1.07 a	-1.10 a	-1.02 a	-1.06 a
	218	-1.05 b	-1.12 a	-1.02 a	-1.04 a
	234	-1.02 b	-1.10 a	-0.95 b	-1.06 a

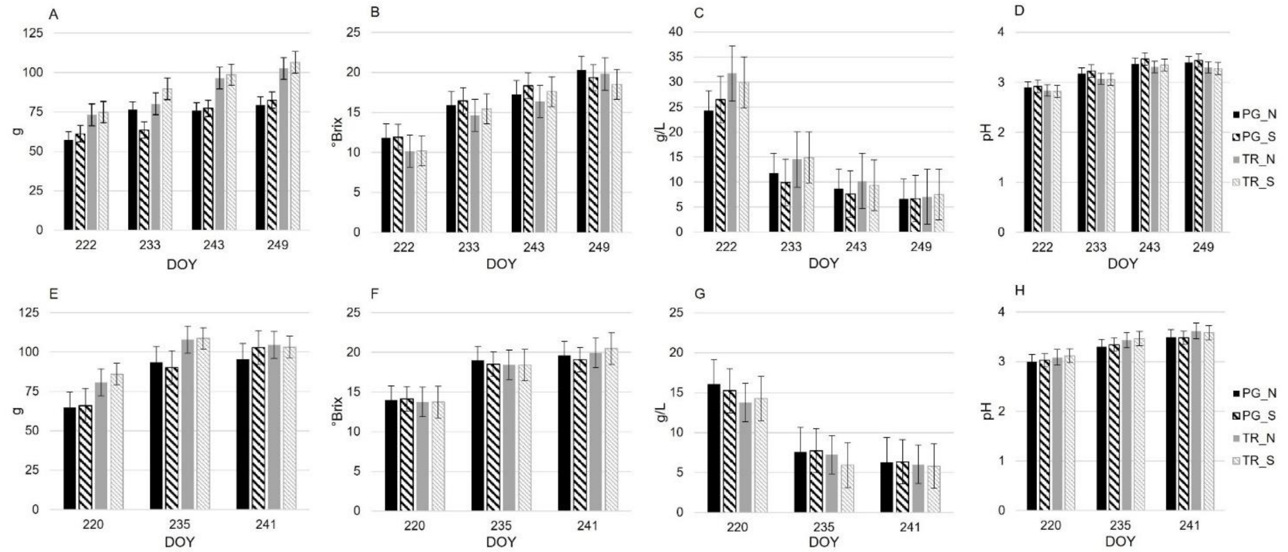

Fig. 6. Seasonal evolution of grape berry composition in 2023 (panels A-D) and 2024 (panels E-H) for the four vineyard sectors: PG_N, PG_S, TR_N, and TR_S. Each bar represents the mean of measurements from 50 berries per vine (n = 20 vines per sector), and error bars indicate the standard error of the mean (SEM). Panels show: (A, E) berry weight (g), (B, F) total soluble solids (°Brix), (C, G) titratable acidity (g L^{-1}), and pH (D, H).

Soil-plant-atmosphere interactions

The relationship between VPD, ESW and NDVI are further analyzed to identify possible interactions among these variables (Fig. 7 A, B). The relationship between ESW and VPD (Fig. 7 A, B) exhibited a clear non-linear pattern in both seasons, with ESW decreasing as VPD increased, reflecting the progressive depletion of extractable soil water under higher evaporative demand. This inverse relationship was well captured by the fitted curves, with determination coefficients (R^2 = 0.63 in 2023; R^2 = 0.66 in 2024) indicating that a substantial portion of ESW variability was explained by atmospheric demand. The NDVI gradient, shown by the color scale, further revealed how canopy vigor co-varied with these dynamics: higher NDVI values corresponded to intermediate ESW and lower VPD, highlighting periods of balanced water availability, while lower NDVI values occurred under higher evaporative conditions.

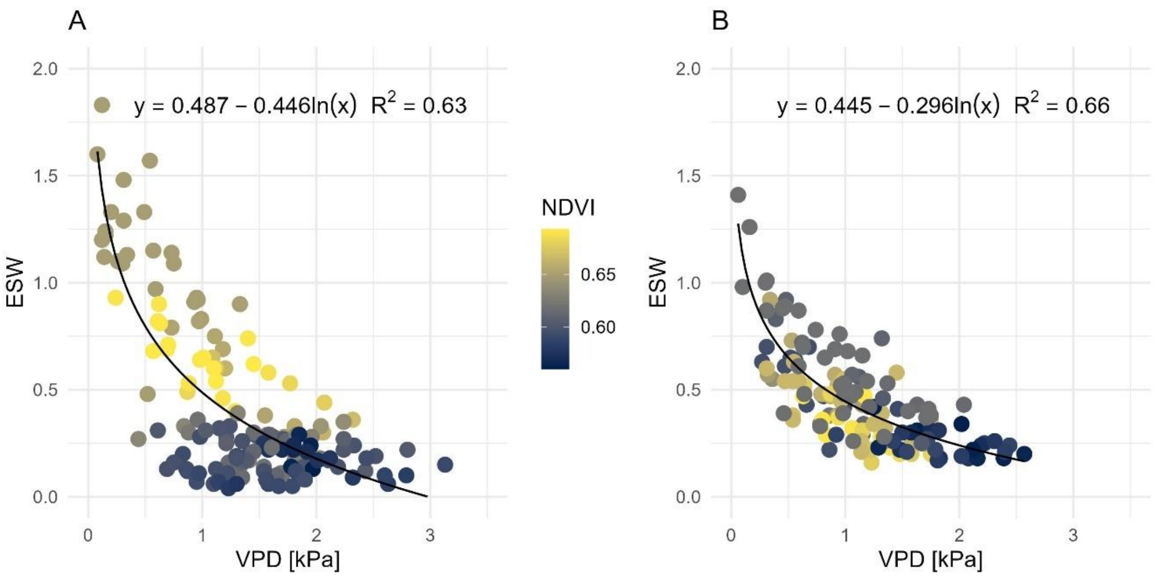

Fig. 7 Relationship between vapor pressure deficit (VPD) and extractable soil water (ESW) for the 2023 (A) and 2024 (B) seasons. The regression line highlights the logarithmic relationship between the two variables, and the coefficients of determination were fitted for both 2023 and 2024 (R^2 = 0.63 and 0.66, respectively). Point colors represent the normalized difference vegetation index (NDVI).

A Principal Component Analysis (PCA) was carried out using ESW, VPD, NDVI, and the average values of midday Ψ_{stem}, TSS and TA for the two monitored grapevine varieties during the 2023 and 2024 seasons (Fig. 8 A, B). In 2023 (Fig. 8 A), the first two components explained 65.1% of the total variance (PC1: 46.0%, PC2: 19.1%). PC1 was dominated by berry composition traits, with strong and opposite loadings of TSS and TA, while VPD contributed negatively along the same axis. This pattern indicates that the ripening process was inversely related to atmospheric evaporative demand. PC2 was mainly driven by NDVI and, to a lesser extent, by VPD and Ψ_{stem}, suggesting a secondary gradient linked to canopy vigor and vine water status. The overall distribution of the two varieties revealed a relatively homogeneous pattern, consistent with the moderate water stress and uniform ripening conditions recorded in 2023. The functional grouping of variables further supports this interpretation: the environmental ellipse was positioned near the center of the biplot, reflecting the buffering effect of adequate soil water availability and irrigation, whereas the physiological ellipse extended along the PC1 axis, illustrating the dominant role of ripening dynamics over climatic influence during this season. In contrast, the 2024 PCA (Fig. 8 B) explained 81.5% of the total variance (PC1: 55.8%, PC2: 25.7%), showing a clearer separation among variables and between varieties. PC1 was strongly driven by TSS and TA and VPD, indicating a pronounced ripening gradient influenced by atmospheric conditions, and in less extent from ESW. PC2 was mainly determined by Ψ_{stem} and NDVI, with a moderate contribution from ESW, revealing a secondary axis associated with vine water potential and canopy development. Compared with 2023, the 2024 biplot showed a tighter coupling between fruit ripening traits and environmental drivers. The relative displacement of the ellipses further emphasized this pattern: the environmental ellipse shifted along PC1, capturing the strong influence of VPD and ESW, while the physiological ellipse extended diagonally across both components, indicating that grape composition traits were more closely linked to Ψ_{stem} and NDVI.

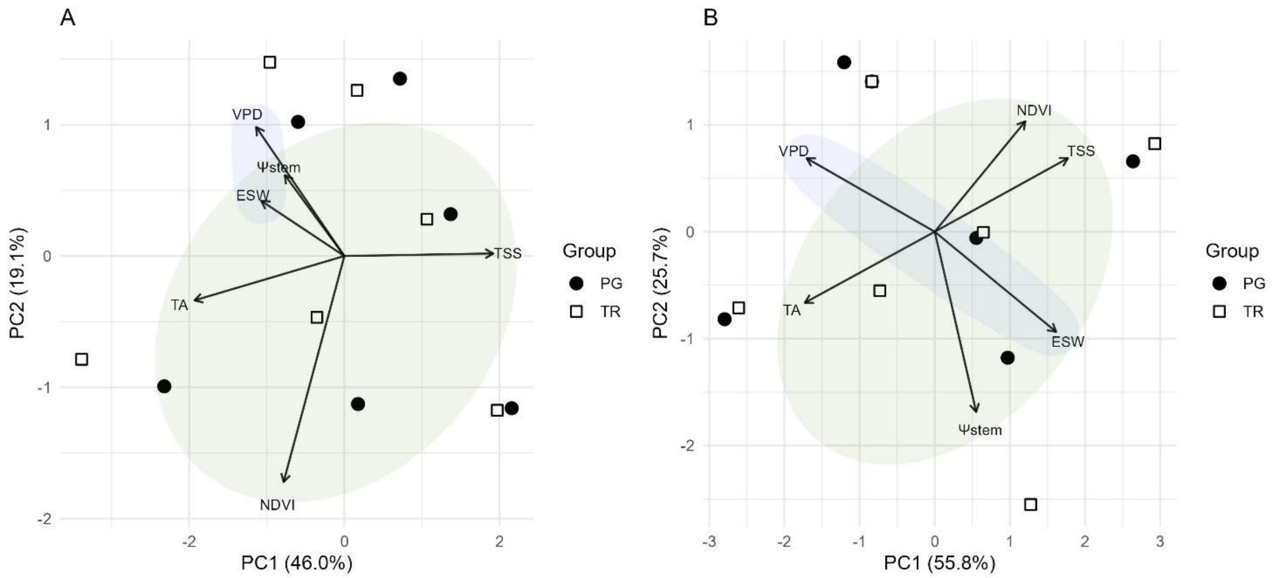

Fig. 8 Principal Component Analysis (PCA) biplots of monitored variables for 2023 (A) and 2024 (B). The analysis was conducted on standardized (z-score) data of extractable soil water (ESW), normalized difference vegetation index (NDVI), vapor pressure deficit (VPD), midday Ψ_{stem} (Ψ_{stem}), total soluble solids (TSS), and titratable acidity (TA). Colored ellipses delineate functional groups of variables: environmental drivers (blue) and physiological/fruit-related traits (green). Each symbol represents the average position of a grapevine variety in the multivariate space: circles correspond to Pignoletto (PG) and squares to Trebbiano Romagnolo (TR). Data from the vineyard sectors were averaged, and the two grapevine varieties are displayed as separate groups.

Discussion and conclusions

This study provided an integrated assessment of soil-plant-atmosphere interactions in a commercial vineyard, combining soil texture characterization, remote sensing indicators (NDVI), vine physiology, and grape composition across two contrasting seasons.

The spatial pattern of soil texture (Fig. 3) indicated clear differences in soil water-holding capacity, with clay-rich zones likely providing greater moisture retention and sandier areas promoting faster drainage. Such within-field variability can influence soil water dynamics and vine water status even over short distances (Brillante et al., 2018; Tang et al., 2022). Soil texture strongly determines soil hydraulic properties and thus grapevine hydraulics (Lavoie-Lamoureux et al., 2017; Tramontini et al., 2013). Because soil properties can vary markedly within a single vineyard, they play a key role in vine performance through growth and water supply (Arnó et al., 2012; Gatti et al., 2022). The spatial and temporal patterns of SWC derived from portable TDR measurements were consistent across seasons and with soil texture variability, showing coherent patterns despite differences in mean SWC levels. NDVI and its inter-annual relative standard deviation (Fig. 4) provided complementary information on intra-field variability and its linkage with soil properties. The overall stability of NDVI values between years suggests that canopy vigor remained relatively uniform, with minor differences likely associated with seasonal soil water availability and atmospheric conditions rather than major changes in vegetation cover. Considering canopy spatial dynamics together with edaphic data reinforces the rationale for zone-specific management approaches in vineyards (Alliaume et al., 2024; von Hebel et al., 2021). Despite temporal fluctuations, the spatial variability of vine water status within the vineyard remained limited across both seasons, likely due to the homogenizing effect of irrigation. Given the stability of soil properties and the fixed irrigation layout, this uniformity is not expected to change substantially over short time scales. Consequently, a single, dedicated survey may be sufficient to characterize the spatial variability and to delineate potential management zones within the vineyard.

In contrast, temporal variability was more pronounced, reflecting differences in rainfall and atmospheric demand between seasons and requiring a precise temporal assessment. The combined monitoring of ESW, NDVI, and VPD effectively captured these temporal dynamics, showing how soil water availability, canopy vigor, and atmospheric demand interact throughout the growing cycle. Incorporating CRNS-derived ESW allowed the seasonal evolution of soil water availability to be linked directly with atmospheric demand and vine response. The relationship between VPD and ESW in both years highlighted a strong coupling between atmospheric demand and soil water dynamics: as VPD increased, ESW declined non-linearly, reflecting progressive depletion of available water under higher evaporative demand. This pattern agrees with previous observations in other agro-ecosystems, where increasing VPD exerts dominant control on soil-plant water fluxes (Novick et al., 2016; J. Zhang et al., 2021). The negative association between VPD and ESW observed across both years (Singh and Apurv, 2025), together with the relatively high coefficients of determination (R^2 = 0.63-0.66), confirms that atmospheric demand was a primary driver of vineyard water dynamics. Seasonal contrasts further illustrated this control. In 2023, abundant early rainfall and timely irrigation buffered vines against evaporative demand, leading to moderate water stress (Ψ_{stem} = -0.66 to -1.06 MPa) and a steady ripening progression with limited varietal differentiation. In 2024, lower soil water availability and higher VPD resulted in more negative Ψ_{stem} values (-0.95 to -1.12 MPa), and an earlier harvest (DOY 241 vs 249 in 2023). Sampling followed phenological development from veraison to harvest, revealing that atmospheric drivers, especially VPD, exerted a stronger influence on ripening in 2024, consistent with earlier findings linking elevated VPD and temperature to faster sugar accumulation and acid degradation (Di Carlo et al., 2019; Fila et al., 2014; Jones et al., 2005; Menzel, 2005; Petrie and Sadras, 2008). The slightly earlier plateau in 2024 indicates that ripening was not delayed despite the shorter season, potentially due to higher VPD, which is closely linked to elevated air temperatures and known to accelerate sugar accumulation (Mira de Orduña, 2010; Sadras and Petrie, 2011). Besides, higher temperature and VPD may have promoted the degradation of organic acids, as described by Rienth et al. (2016). This could explain why, despite the earlier harvest in 2024, titratable acidity levels at harvest were comparable between years (Fig. 9 C, G).

The PCA analysis confirmed these contrasting seasonal controls. In 2023, variance was mainly driven by berry ripening traits that were largely decoupled from atmospheric variables, whereas in 2024, environmental drivers (ESW, VPD) were more closely linked to physiological traits, underscoring a stronger climatic influence on vine functioning. This divergence indicates that under conditions of high evaporative demand and adequate soil water supply, vine physiology and ripening become increasingly responsive to atmospheric drivers, partially overriding the buffering role of SWC. Despite the restricted number of variables included in the PCA, these findings are consistent with previous studies showing that soil-plant-atmosphere interactions exert cascading effects on vine physiology and fruit composition (Beauchet et al., 2020; Suter et al., 2019; Yu et al., 2020) and that intra-block variability in water status affects berry development (Jasse et al., 2021). In this case, however, such effects were modest, likely due to irrigation maintaining generally adequate water availability.

Overall, this study proved how CRNS-derived SWC is a robust integrative indicator of soil-plant water relations and a valuable complement to plant-based and remote-sensing observations. As such, this integration can offer a non-invasive solution to enhance the temporal and functional understanding of crop water relations, supporting more adaptive and sustainable water management. Future work should extend this approach to other crops, incorporate additional physiological variables, and explore CRNS scalability within decision-support systems.

Acknowledgements

The authors gratefully acknowledge Societa Agricola CACI (Imola, Bologna, Italy) for their permission to conduct the trial.

Conflict of interest

The authors declare no conflicts of interest. The funders had no role in the design of the study; in the collection, analyses, or interpretation of data; in the writing of the manuscript, or in the decision to publish the results.

Contributions

Conceptualization and methodology: R.M., I.F. and G.B.; validation, formal analysis, and investigation: R.M., F.V., M.B. and G.B.; writing-original draft: R.M., F.V. and M.B.; writing-review and supervision: I.F. and G.B. All authors have read and agreed to the published version of the manuscript.

Data availability statement

The dataset including CRNS data, precipitation, irrigation records, air temperature, and relative humidity analyzed in this study is publicly available on Zenodo under the title "Datasets analyzed within the study *Cosmic-ray neutron sensing to monitor soil moisture across various irrigation methods*" at Mazzoleni et al. (2025b). This dataset is associated with the publication "Cosmic-ray neutron sensing to monitor soil moisture across various irrigation methods", which is available at the time of submission as a preprint (Mazzoleni et al., 2025a).

Funding

This research is part of the PhD scholarship funded by NextGenEU - DM352 and Finapp S.p.A.

References

Acevedo-Opazo, C., Ortega-Farias, S., & Fuentes, S. (2010). Effects of grapevine (*Vitis vinifera* L.) water status on water consumption, vegetative growth and grape quality: An irrigation scheduling application to achieve regulated deficit irrigation. *Agricultural Water Management*, *97*(7), 956–964. https://doi.org/10.1016/j.agwat.2010.01.025

Allegro, G., Pastore, C., Valentini, G., Mazzoleni, R., & Filippetti, I. (2023). Irrigation during ripening may reduce sunburn damages on berries of *Vitis vinifera* L. 'Sangiovese.' *Acta Horticulturae*, *1366*, 377–384. https://doi.org/10.17660/ActaHortic.2023.1366.46

Allen, R. G., Pereira, L., Raes, D., & Smith, M. (Eds.). (1998). *Crop evapotranspiration: Guidelines for computing crop water requirements* (repr). Food and Agriculture Organization of the United Nations.

Alliaume, F., Echeverria, G., Ferrer, M., & González Barrios, P. (2024). A Study of the Multivariate Spatial Variability of Soil Properties, and their Association with Vine Vigor Growing on a Clayish Soil. *Journal of Soil Science and Plant Nutrition*, *24*(2), 3282–3297. https://doi.org/10.1007/s42729-024-01751-8

Antolini, G., Auteri, L., Pavan, V., Tomei, F., Tomozeiu, R., & Marletto, V. (2016). A daily high-resolution gridded climatic data set for Emilia-Romagna, Italy, during 1961-2010: EMILIA-ROMAGNA DAILY GRIDDED CLIMATIC DATA SET. *International Journal of Climatology*, *36*(4), 1970–1986. https://doi.org/10.1002/joc.4473

Arnó, J., Rosell, J. R., Blanco, R., Ramos, M. C., & Martínez-Casasnovas, J. A. (2012). Spatial variability in grape yield and quality influenced by soil and crop nutrition characteristics. *Precision Agriculture*, *13*(3), 393–410. https://doi.org/10.1007/s11119-011-9254-1

Babaeian, E., Sadeghi, M., Jones, S. B., Montzka, C., Vereecken, H., & Tuller, M. (2019). Ground, Proximal, and Satellite Remote Sensing of Soil Moisture. *Reviews of Geophysics*, *57*(2), 530–616. https://doi.org/10.1029/2018RG000618

Baetens, L., Desjardins, C., & Hagolle, O. (2019). Validation of Copernicus Sentinel-2 Cloud Masks Obtained from MAJA, Sen2Cor, and FMask Processors Using Reference Cloud Masks Generated with a Supervised Active Learning Procedure. *Remote Sensing*, *11*(4), 433. https://doi.org/10.3390/rs11040433

Beauchet, S., Cariou, V., Renaud-Gentie, C., Meunier, M., Siret, R., Thiollet-Scholtus, M., & Jourjon, F. (2020). Modeling grape quality by multivariate analysis of viticulture practices, soil and climate. *OENO One*. https://doi.org/10.20870/oeno-one....1067

Bolognini, M., Modina, D., Bianchi, D., Cavallaro, L., Carnevali, P., & Brancadoro, L. (2023). Using a vegetation index to define homogeneous zones for variable rate irrigation in vineyard. In *Precision agriculture '23* (pp. 75–82). Wageningen Academic. https://doi.org/10.3920/978-90-8686-947-3_7

Bonada, M., Petrie, P. R., Phogat, V., Collins, C., & Sadras, V. O. (2023). Benchmarking Water-Limited Yield Potential and Yield Gaps of Shiraz in the Barossa and Eden Valleys. *Australian Journal of Grape and Wine Research*, *2023*(1), 5807266. https://doi.org/10.1155/2023/5807266

Brillante, L., Mathieu, O., Lévêque, J., van Leeuwen, C., & Bois, B. (2018). Water status and must composition in grapevine cv. Chardonnay with different soils and topography and a mini meta-analysis of the δ13C/water potentials correlation. *Journal of the Science of Food and Agriculture*, *98*(2), 691–697. https://doi.org/10.1002/jsfa.8516

Brogi, C., Pisinaras, V., Köhli, M., Dombrowski, O., Hendricks Franssen, H.-J., Babakos, K., Chatzi, A., Panagopoulos, A., & Bogena, H. R. (2023). Monitoring Irrigation in Small Orchards with Cosmic-Ray Neutron Sensors. *Sensors*, *23*(5), Article 5. https://doi.org/10.3390/s23052378

Büntgen, U., Reinig, F., Verstege, A., Piermattei, A., Kunz, M., Krusic, P., Slavin, P., Štěpánek, P., Torbenson, M., del Castillo, E. M., Arosio, T., Kirdyanov, A., Oppenheimer, C., Trnka, M., Palosse, A., Bebchuk, T., Camarero, J. J., & Esper, J. (2024). Recent summer warming over the western Mediterranean region is unprecedented since medieval times. *Global and Planetary Change*, *232*, 104336. https://doi.org/10.1016/j.gloplacha.2023.104336

Bwambale, E., Abagale, F. K., & Anornu, G. K. (2022). Smart irrigation monitoring and control strategies for improving water use efficiency in precision agriculture: A review. *Agricultural Water Management*, *260*, 107324. https://doi.org/10.1016/j.agwat.2021.107324

Chaves, M. M., Zarrouk, O., Francisco, R., Costa, J. M., Santos, T., Regalado, A. P., Rodrigues, M. L., & Lopes, C. M. (2010). Grapevine under deficit irrigation: Hints from physiological and molecular data. *Annals of Botany*, *105*(5), 661–676. https://doi.org/10.1093/aob/mcq030

Desilets, D., Zreda, M., & Ferré, T. P. A. (2010). Nature's neutron probe: Land surface hydrology at an elusive scale with cosmic rays. *Water Resources Research*, *46*(11). https://doi.org/10.1029/2009WR008726

Di Carlo, P., Aruffo, E., & Brune, W. H. (2019). Precipitation intensity under a warming climate is threatening some Italian premium wines. *Science of The Total Environment*, *685*, 508–513. https://doi.org/10.1016/j.scitotenv.2019.05.449

Fila, G., Gardiman, M., Belvini, P., Meggio, F., & Pitacco, A. (2014). A comparison of different modelling solutions for studying grapevine phenology under present and future climate scenarios. *Agricultural and Forest Meteorology*, *195–196*, 192–205. https://doi.org/10.1016/j.agrformet.2014.05.011

Franz, T. E., Zreda, M., Rosolem, R., & Ferre, T. P. A. (2012). Field Validation of a Cosmic-Ray Neutron Sensor Using a Distributed Sensor Network. *Vadose Zone Journal*, *11*(4). https://doi.org/10.2136/vzj2012.0046

Fuentes, S., & Gago, J. (2022). Chapter 7—Modern approaches to precision and digital viticulture. In J. M. Costa, S. Catarino, J. M. Escalona, & P. Comuzzo (Eds.), *Improving Sustainable Viticulture and Winemaking Practices* (pp. 125–145). Academic Press. https://doi.org/10.1016/B978-0-323-85150-3.00015-3

Gatti, M., Garavani, A., Squeri, C., Diti, I., De Monte, A., Scotti, C., & Poni, S. (2022). Effects of intra-vineyard variability and soil heterogeneity on vine performance, dry matter and nutrient partitioning. *Precision Agriculture*, *23*(1), 150–177. https://doi.org/10.1007/s11119-021-09831-w

Gerakis, A., & Zalidis, G. (1998). Estimating field-measured, plant extractable water from soil properties: Beyond statistical models. *Irrigation and Drainage Systems*, *12*, 311–322.

Gianessi, S., Polo, M., Stevanato, L., Lunardon, M., Francke, T., Oswald, S. E., Said Ahmed, H., Toloza, A., Weltin, G., Dercon, G., Fulajtar, E., Heng, L., & Baroni, G. (2024). Testing a novel sensor design to jointly measure cosmic-ray neutrons, muons and gamma rays for non-invasive soil moisture estimation. *Geoscientific Instrumentation, Methods and Data Systems*, *13*(1), 9–25. https://doi.org/10.5194/gi-13-9-2024

Giovos, R., Tassopoulos, D., Kalivas, D., Lougkos, N., & Priovolou, A. (2021). Remote Sensing Vegetation Indices in Viticulture: A Critical Review. *Agriculture*, *11*(5), Article 5. https://doi.org/10.3390/agriculture11050457

Grolemund, G., & Wickham, H. (2011). Dates and Times Made Easy with lubridate. *Journal of Statistical Software*, *40*, 1–25. https://doi.org/10.18637/jss.v040.i03

Jasse, A., Berry, A., Aleixandre-Tudo, J. L., & Poblete-Echeverría, C. (2021). Intra-block spatial and temporal variability of plant water status and its effect on grape and wine parameters. *Agricultural Water Management*, *246*, 106696. https://doi.org/10.1016/j.agwat.2020.106696

Jones, G. V., White, M. A., Cooper, O. R., & Storchmann, K. (2005). Climate Change and Global Wine Quality. *Climatic Change*, *73*(3), 319–343. https://doi.org/10.1007/s10584-005-4704-2

Kassambara, A., & Mundt, F. (2016). *factoextra: Extract and Visualize the Results of Multivariate Data Analyses*. https://rpkgs.datanovia.com/factoextra/index.html

Köhli, M., Schrön, M., Zreda, M., Schmidt, U., Dietrich, P., & Zacharias, S. (2015). Footprint characteristics revised for field-scale soil moisture monitoring with cosmic-ray neutrons. *Water Resources Research*, *51*(7), 5772–5790. https://doi.org/10.1002/2015WR017169

Lavoie-Lamoureux, A., Sacco, D., Risse, P.-A., & Lovisolo, C. (2017). Factors influencing stomatal conductance in response to water availability in grapevine: A meta-analysis. *Physiologia Plantarum*, *159*(4), 468–482. https://doi.org/10.1111/ppl.12530

Lê, S., Josse, J., & Husson, F. (2008). FactoMineR: An R Package for Multivariate Analysis. *Journal of Statistical Software*, *25*, 1–18. https://doi.org/10.18637/jss.v025.i01

Lebon, E., Dumas, V., Pieri, P., & Schultz, H. R. (2003). Modelling the seasonal dynamics of the soil water balance of vineyards. *Functional Plant Biology*, *30*(6), 699. https://doi.org/10.1071/FP02222

Li, D., Schrön, M., Köhli, M., Bogena, H., Weimar, J., Jiménez Bello, M. A., Han, X., Martínez Gimeno, M. A., Zacharias, S., Vereecken, H., & Hendricks Franssen, H. (2019). Can Drip Irrigation be Scheduled with Cosmic-Ray Neutron Sensing? *Vadose Zone Journal*, *18*(1), 190053. https://doi.org/10.2136/vzj2019.05.0053

Lorenz, D. h., Eichhorn, K. w., Bleiholder, H., Klose, R., Meier, U., & Weber, E. (1995). Growth Stages of the Grapevine: Phenological growth stages of the grapevine (Vitis vinifera L. ssp. vinifera)—Codes and descriptions according to the extended BBCH scale. *Australian Journal of Grape and Wine Research*, *1*(2), 100–103. https://doi.org/10.1111/j.1755-0238.1995.tb00085.x

Lovisolo, C., Perrone, I., Carra, A., Ferrandino, A., Flexas, J., Medrano, H., & Schubert, A. (2010). Drought-induced changes in development and function of grapevine (Vitis spp.) organs and in their hydraulic and non-hydraulic interactions at the whole-plant level: A physiological and molecular update. *Functional Plant Biology*, *37*(2), 98–116. https://doi.org/10.1071/FP09191

Massari, C., Modanesi, S., Dari, J., Gruber, A., De Lannoy, G. J. M., Girotto, M., Quintana-Seguí, P., Le Page, M., Jarlan, L., Zribi, M., Ouaadi, N., Vreugdenhil, M., Zappa, L., Dorigo, W., Wagner, W., Brombacher, J., Pelgrum, H., Jaquot, P., Freeman, V., … Brocca, L. (2021). A Review of Irrigation Information Retrievals from Space and Their Utility for Users. *Remote Sensing*, *13*(20), 4112. https://doi.org/10.3390/rs13204112

Mazzoleni, R., Emamalizadeh, S., & Baroni, G. (2025a). *Cosmic-ray neutron sensing to monitor soil moisture across various irrigation methods* (Preprint No. VZJ-2025-06-0057-OA.R1). ESS Open Archive. https://doi.org/10.22541/essoar.176097443.35022248/v1

Mazzoleni, R., Emamalizadeh, S., & Baroni, G. (2025b). *Datasets analyzed within the study "Cosmic-ray neutron sensing to monitor soil moisture across various irrigation methods"* [Dataset]. Zenodo. https://doi.org/10.5281/ZENODO.17177047

Menzel, A. (2005). A 500 year pheno-climatological view on the 2003 heatwave in Europe assessed by grape harvest dates. *Meteorologische Zeitschrift*, *14*(1), 75–77. https://doi.org/10.1127/0941-2948/2005/0014-0075

Mira de Orduña, R. (2010). Climate change associated effects on grape and wine quality and production. *Food Research International*, *43*(7), 1844–1855. https://doi.org/10.1016/j.foodres.2010.05.001

Novick, K. A., Ficklin, D. L., Stoy, P. C., Williams, C. A., Bohrer, G., Oishi, A. C., Papuga, S. A., Blanken, P. D., Noormets, A., Sulman, B. N., Scott, R. L., Wang, L., & Phillips, R. P. (2016). The increasing importance of atmospheric demand for ecosystem water and carbon fluxes. *Nature Climate Change*, *6*(11), 1023–1027. https://doi.org/10.1038/nclimate3114

Ortuani, B., Mayer, A., Bianchi, D., Sona, G., Crema, A., Modina, D., Bolognini, M., Brancadoro, L., Boschetti, M., & Facchi, A. (2024). Effectiveness of Management Zones Delineated from UAV and Sentinel-2 Data for Precision Viticulture Applications. *Remote Sensing*, *16*(4), 635. https://doi.org/10.3390/rs16040635

Palazzi, F., Biddoccu, M., Borgogno Mondino, E. C., & Cavallo, E. (2023). Use of Remotely Sensed Data for the Evaluation of Inter-Row Cover Intensity in Vineyards. *Remote Sensing*, *15*(1), 41. https://doi.org/10.3390/rs15010041

Pellegrino, A., Lebon, E., Voltz, M., & Wery, J. (2005). Relationships between plant and soil water status in vine (Vitis vinifera L.). *Plant and Soil*, *266*(1), 129–142. https://doi.org/10.1007/s11104-005-0874-y

Pereyra, G., Pellegrino, A., Gaudin, R., & Ferrer, M. (2022). Evaluation of site-specific management to optimise *Vitis vinifera* L. (cv. Tannat) production in a vineyard with high heterogeneity. *OENO One*, *56*(3), Article 3. https://doi.org/10.20870/oeno-one.2022.56.3.5485

Petrie, P. r., & Sadras, V. o. (2008). Advancement of grapevine maturity in Australia between 1993 and 2006: Putative causes, magnitude of trends and viticultural consequences. *Australian Journal of Grape and Wine Research*, *14*(1), 33–45. https://doi.org/10.1111/j.1755-0238.2008.00005.x

Rienth, M., Torregrosa, L., Sarah, G., Ardisson, M., Brillouet, J.-M., & Romieu, C. (2016). Temperature desynchronizes sugar and organic acid metabolism in ripening grapevine fruits and remodels their transcriptome. *BMC Plant Biology*, *16*(1), 164. https://doi.org/10.1186/s12870-016-0850-0

Robinson, D. A., Campbell, C. S., Hopmans, J. W., Hornbuckle, B. K., Jones, S. B., Knight, R., Ogden, F., Selker, J., & Wendroth, O. (2008). Soil Moisture Measurement for Ecological and Hydrological Watershed-Scale Observatories: A Review. *Vadose Zone Journal*, *7*(1), 358–389. https://doi.org/10.2136/vzj2007.0143

Sadras, V. o., & Petrie, P. r. (2011). Quantifying the onset, rate and duration of sugar accumulation in berries from commercial vineyards in contrasting climates of Australia. *Australian Journal of Grape and Wine Research*, *17*(2), 190–198. https://doi.org/10.1111/j.1755-0238.2011.00135.x

Schrön, M., Köhli, M., Scheiffele, L., Iwema, J., Bogena, H. R., Lv, L., Martini, E., Baroni, G., Rosolem, R., Weimar, J., Mai, J., Cuntz, M., Rebmann, C., Oswald, S. E., Dietrich, P., Schmidt, U., & Zacharias, S. (2017). Improving calibration and validation of cosmic-ray neutron sensors in the light of spatial sensitivity. *Hydrology and Earth System Sciences*, *21*(10), 5009–5030. https://doi.org/10.5194/hess-21-5009-2017

Seager, R., Liu, H., Henderson, N., Simpson, I., Kelley, C., Shaw, T., Kushnir, Y., & Ting, M. (2014). Causes of Increasing Aridification of the Mediterranean Region in Response to Rising Greenhouse Gases. *Journal of Climate*, *27*(12), 4655–4676. https://doi.org/10.1175/JCLI-D-13-00446.1

Seneviratne, S. I., Corti, T., Davin, E. L., Hirschi, M., Jaeger, E. B., Lehner, I., Orlowsky, B., & Teuling, A. J. (2010). Investigating soil moisture–climate interactions in a changing climate: A review. *Earth-Science Reviews*, *99*(3), 125–161. https://doi.org/10.1016/j.earscirev.2010.02.004

Singh, V., & Apurv, T. (2025). An Analytical Approach for Quantifying the Role of Vapor Pressure Deficit in Soil Moisture Depletion During Flash Droughts. *Water Resources Research*, *61*(6), e2024WR038995. https://doi.org/10.1029/2024WR038995

Soulis, K. X., Elmaloglou, S., & Dercas, N. (2015). Investigating the effects of soil moisture sensors positioning and accuracy on soil moisture based drip irrigation scheduling systems. *Agricultural Water Management*, *148*, 258–268. https://doi.org/10.1016/j.agwat.2014.10.015

Stevanato, L., Baroni, G., Cohen, Y., Fontana, C. L., Gatto, S., Lunardon, M., Marinello, F., Moretto, S., & Morselli, L. (2019). A Novel Cosmic-Ray Neutron Sensor for Soil Moisture Estimation over Large Areas. *Agriculture*, *9*(9), Article 9. https://doi.org/10.3390/agriculture9090202

Susha Lekshmi, S. U., Singh, D. N., & Shojaei Baghini, M. (2014). A critical review of soil moisture measurement. *Measurement*, *54*, 92–105. https://doi.org/10.1016/j.measurement.2014.04.007

Suter, B., Triolo, R., Pernet, D., Dai, Z., & Van Leeuwen, C. (2019). Modeling Stem Water Potential by Separating the Effects of Soil Water Availability and Climatic Conditions on Water Status in Grapevine (Vitis vinifera L.). *Frontiers in Plant Science*, *10*. https://doi.org/10.3389/fpls.2019.01485

Szabó, B., Weynants, M., & Weber, T. K. D. (2021). Updated European hydraulic pedotransfer functions with communicated uncertainties in the predicted variables (euptfv2). *Geoscientific Model Development*, *14*(1), 151–175. https://doi.org/10.5194/gmd-14-151-2021

Tang, Z., Jin, Y., Alsina, M. M., McElrone, A. J., Bambach, N., & Kustas, W. P. (2022). Vine water status mapping with multispectral UAV imagery and machine learning. *Irrigation Science*, *40*(4), 715–730. https://doi.org/10.1007/s00271-022-00788-w

Tramontini, S., van Leeuwen, C., Domec, J.-C., Destrac-Irvine, A., Basteau, C., Vitali, M., Mosbach-Schulz, O., & Lovisolo, C. (2013). Impact of soil texture and water availability on the hydraulic control of plant and grape-berry development. *Plant and Soil*, *368*(1), 215–230. https://doi.org/10.1007/s11104-012-1507-x

Valentini, G., Pastore, C., Allegro, G., Mazzoleni, R., Chinnici, F., & Filippetti, I. (2022). Vine Physiology, Yield Parameters and Berry Composition of Sangiovese Grape under Two Different Canopy Shapes and Irrigation Regimes. *Agronomy*, *12*(8), Article 8. https://doi.org/10.3390/agronomy12081967

Velazquez-Chavez, L. J., Daccache, A., Mohamed, A. Z., & Centritto, M. (2024). Plant-based and remote sensing for water status monitoring of orchard crops: Systematic review and meta-analysis. *Agricultural Water Management*, *303*, 109051. https://doi.org/10.1016/j.agwat.2024.109051

von Hebel, C., Reynaert, S., Pauly, K., Janssens, P., Piccard, I., Vanderborght, J., van der Kruk, J., Vereecken, H., & Garré, S. (2021). Toward high-resolution agronomic soil information and management zones delineated by ground-based electromagnetic induction and aerial drone data. *Vadose Zone Journal*, *20*(4), e20099. https://doi.org/10.1002/vzj2.20099

Wickham, H. (2011). Ggplot2. *WIREs Computational Statistics*, *3*(2), 180–185. https://doi.org/10.1002/wics.147

Yu, R., Brillante, L., Martínez-Lüscher, J., & Kurtural, S. K. (2020). Spatial Variability of Soil and Plant Water Status and Their Cascading Effects on Grapevine Physiology Are Linked to Berry and Wine Chemistry. *Frontiers in Plant Science*, *11*. https://doi.org/10.3389/fpls.2020.00790

Zhang, J., Guan, K., Peng, B., Pan, M., Zhou, W., Jiang, C., Kimm, H., Franz, T. E., Grant, R. F., Yang, Y., Rudnick, D. R., Heeren, D. M., Suyker, A. E., Bauerle, W. L., & Miner, G. L. (2021). Sustainable irrigation based on co-regulation of soil water supply and atmospheric evaporative demand. *Nature Communications*, *12*(1), 5549. https://doi.org/10.1038/s41467-021-25254-7

Zhang, Y., Oren, R., & Kang, S. (2012). Spatiotemporal variation of crown-scale stomatal conductance in an arid Vitis vinifera L. cv. Merlot vineyard: Direct effects of hydraulic properties and indirect effects of canopy leaf area. *Tree Physiology*, *32*(3), 262–279. https://doi.org/10.1093/treephys/tpr120

Zhou, S., Zhang, Y., Park Williams, A., & Gentine, P. (2019). Projected increases in intensity, frequency, and terrestrial carbon costs of compound drought and aridity events. *Science Advances*, *5*(1), eaau5740. https://doi.org/10.1126/sciadv.aau5740

Zreda, M., Desilets, D., Ferré, T. P. A., & Scott, R. L. (2008). Measuring soil moisture content non-invasively at intermediate spatial scale using cosmic-ray neutrons. *Geophysical Research Letters*, *35*(21). https://doi.org/10.1029/2008GL035655

Zreda, M., Shuttleworth, W. J., Zeng, X., Zweck, C., Desilets, D., Franz, T., & Rosolem, R. (2012). COSMOS: The COsmic-ray Soil Moisture Observing System. *Hydrology and Earth System Sciences*, *16*(11), 4079–4099. https://doi.org/10.5194/hess-16-4079-2012